Frequency Selective Surface with High Selectivity by Adding an Inductive Layer

Muaad Hussein, Zhenghua Tang, Yi Huang and Jiafeng Zhou

***Abstract*— A Frequency Selective Surfaces (FSS) is essentially a spatial filter. Compared to a connectorized traditional filter with fixed ports, an FSS can separate signals at different frequencies by both transmission and reflection. In this paper, we propose an approach to design FSSs with high selectivity. This is achieved by adding an inductive surface on the other side of a resonant surface.**

The proposed FSS will have both a passband and a stopband. Such a response has two advantages. One is that by choosing the frequencies properly, the stopband can improve the selectivity of the passband significantly, and vice versa. Another advantage is that the proposed FSS can operate effectively as a diplexer by separating signals at the passband and stopband.

The center frequency and bandwidth of the passband and stopband can be independently designed. The proposed FSS has a small element size, low profile and insensitive response to surrounding dielectric materials. The proposed design method has many potential applications. An FSS has been fabricated and tested. Experimental results have validated the proposed theory and design method.

Index Terms: **Frequency selective surface (FSS), periodic structures, artificial magnetic conductor (AMC), filter, diplexer**

I. INTRODUCTION

Frequency selective surface (FSSs) are usually constructed by patches, slots or arbitrary geometrical structures within a metallic screen supported by dielectric materials. Characteristics such as the array element type and shape, the presence or absence of dielectric slabs, the dielectric substrate parameters and inter-element spacing will determine the response of the FSS, such as its transfer function, bandwidth, and its dependence on the angular wave (incident and polarization angles). Early researches with respect to FSSs using an infinite planar array [1], a two-layer dipole array [2] or metallic mesh structures [3] focus on the theoretical calculation of scattering or reflection properties when plane electromagnetic waves are incident on the structures. Currently, FSSs have been the subject of intense investigations for a wide range of applications for decades, such as bandpass filters [4-7] and high impedance electromagnetic surfaces [8].

An artificial magnetic conductor (AMC) or high impedance surface (HIS) consists of an FSS placed above a perfect electric conductor (PEC) ground plane, with a dielectric material in between [9]. It displays a 0º reflection coefficient phase at a given frequency [8]. An AMC can be applied to control the propagation of electromagnetic waves in certain patterns. These structures can improve the performance of an antenna [8]. It exhibits selectivity in suppressing surface waves to improve the gain of antennas. A U-slot patch antenna integrated to a modified Jerusalem cross FSS was proposed in [10] to improve the antenna gain, bandwidth and return loss at 2.45 and 5.8 GHz for Bluetooth and WLAN applications. A split-ring shaped slot antenna was integrated to an FSS to enhance the bandwidth and gain of the antenna in [11].

In general, good selectivity characteristics of FSSs refer to the rapid decline of the sideband of the transmission coefficients. Many designs have been reported on the optimization of selectivity of FSSs [12-17]. Such designs include the use of substrate integrated waveguide cavities [12], two layers of metallic unit cells [13], a periodic array of gridded-triple square loop [14], an identical tripole resonators [15] and loop-shaped resonators [16]. The selectivity of FSSs can be enhanced by cascading substrate integrated waveguide cavities [12]. The coupling between capacitive patches in different layers [13] in the FSS can induce a good selection feature. A quad-band FSS [14] can be obtained by cascading three metallic layers to achieve high selectivity. The aperture-coupled resonator structure [15] consisting of identical tripole resonators also exhibits high selectivity.

The target of this study is to propose a low-profile FSS design that shows high selectivity. This is achieved by adding an inductive layer on the other side of a resonant layer. By doing so, both a passband and a stopband can be generated. The two bands can improve the selectivity of each other. Another advantage is that the performance of the FSS is very stable when it is attached to other dielectric material.

An equivalent circuit is derived to analyzed the proposed design. With the equivalent circuit, it was demonstrated that the center frequency and the bandwidth of the passband and the stopband can be synthesized independently. This will provide great flexibility for the design. The FSS also have a small element size and a low profile.

The proposed FSS design has many potential applications. The passband and stopband can be designed so that the FSS can operate as a diplexer to separate signals at these two bands. This is because, for an FSS, both the reflected and the transmitted signals can be utilized. While in a traditional filter, usually only the transmitted signal is utilizable. The insensitivity to surrounding dielectric materials suggests that FSS can be potentially used as part of an AMC to improve the gain of RFID tag antennas. Such applications will be exploited as future work.

In this paper, Section II discusses the equivalent circuit of an FSS. Section III describes the procedure to design the proposed FSS. The experimental setup and measurement results to verify the proposed design method are provided in Section IV. Conclusions and future work are finally described in Section V.

II. EQUIVALENT CIRCUIT OF AN FSS

This section discusses the equivalent circuit of an FSS. In general, at least for mechanical and miniaturization reasons, most FSSs are supported by dielectric slabs. The dielectric materials have strong effect on the bandwidth, resonant

Manuscript received 27 January 2019. The authors are with the Department of Electrical Engineering and Electronics, The University of Liverpool, UK. (e-mail:Jiafeng.Zhou@liverpool.ac.uk).

frequency and element size. FSSs can be classified to two types based on the equivalent circuit: capacitive surfaces and inductive surfaces. It is well known that the equivalent circuit for a patch is a shunt capacitor (C_p), and for a mesh is a shunt inductor (L_i) [3].

For a mesh-type FSS layer, when it is attached to an infinitely wide dielectric material with dielectric constant ε_r, effect of the dielectric material on the FSS can be explained by using the equivalent circuits of the FSS and the dielectric slab. The approximate value of the intrinsic inductance can be calculated using the formula [18]

$$L = \mu_o \mu_e \ (P/2\pi) \ln \csc (\pi w/2P) \quad (1)$$

where P is the strip length and w is the strip width of the meshes. μ_o and μ_e denote the permeability of free space and the effective relative permeability of the structure, respectively.

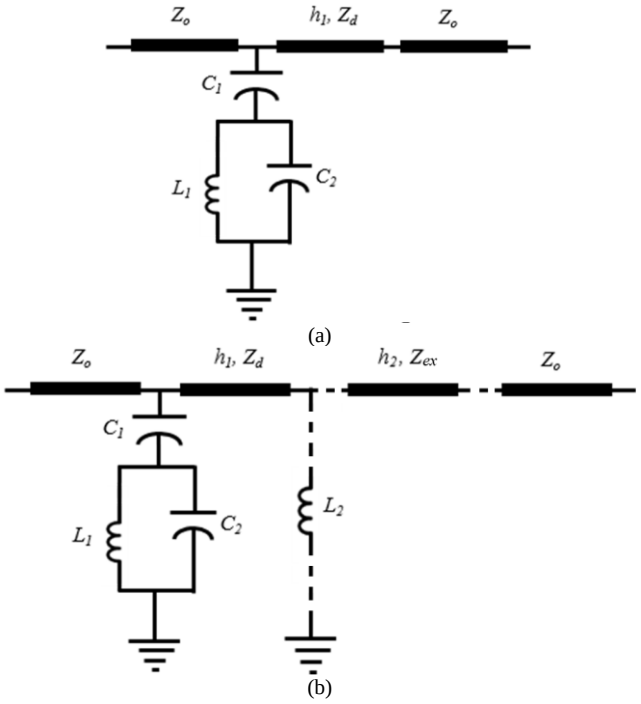

Fig. 1. Equivalent circuit of an FSS (a) without the inductive layer (b) with the inductive layer and also an extra layer of dielectric layer.

The dielectric slab can be represented by a short piece of transmission lines h_1 as shown in Fig. 1. The characteristic impedance of the transmission line is $Z_d = Z_0/\sqrt{\varepsilon_r}$, where Z_0 = 377 Ω is the free space impedance, and ε_r is the effective relative permittivity of the structure.

For a capacitive patch-type FSS, when it is attached an infinitely wide dielectric slab, the equivalent circuit can be obtained using a procedure similar to the one for an inductive FSS. The approximate value of the corresponding equivalent capacitance C_p can be calculated by [18]:

$$C_p = \varepsilon_0 \varepsilon_e \ (2P/\pi) \ln \csc (\pi g/2P) \quad (2)$$

The capacitance is determined by the patch length P, the gap g between adjacent patches and the effective dielectric constant ε_e of the structure.

From (1), it can be noticed that the inductance value of the meshes of the FSS is mainly determined by its strip width. An increase in strip width of the FSS will result in the inductance to be reduced. Similarly, a decrease in the width of the meshes will lead to an increase of the inductance. The changes of the inductive value of the FSS will significantly affecting its characteristic impedance. This will influence the S-parameters of the FSS when electromagnetic waves are incident on the FSS

It can also be observed from above that, when an FSS is attached to a dielectric material, the change in the bandwidth and resonant frequency can be attributed to two reasons. Firstly the dielectric material directly changes the effective dielectric constant of the structure and thereby the intrinsic capacitance. Secondly, it is because the equivalent circuit for the FSS will be changed by adding a series transmission line with a characteristic impedance of Z_d, as shown in Fig. 1(a).

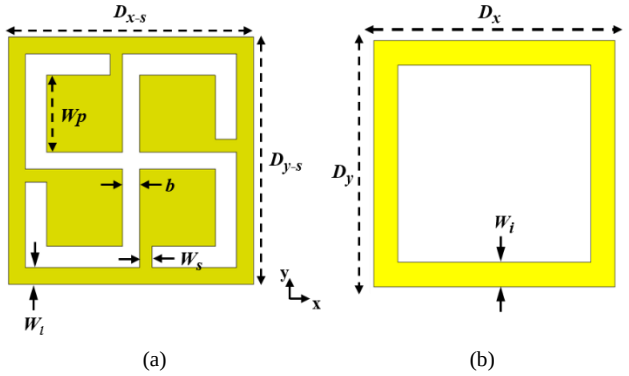

Fig. 2. Structures of (a) the resonant surface and (b) the inductive surface.

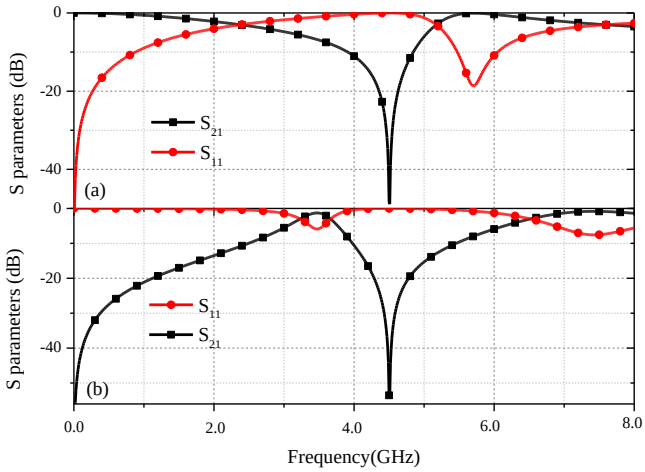

Fig. 3. The calculated S-parameters of (a) the original FSS (resonant surface) without the inductive layer and (B) the proposed FSS with the inductive layer.

III. FSS Circuit Design

The choice of elements is of great importance when designing an FSS. Some structures are inherently narrowband or wideband. Different FSS types can be chosen based on the application requirements. These requirements usually include a level of dependence on the polarization and incidence angle of incoming waves and bandwidth. In general, FSS structures with a small element size, compared to the wavelength, will be in insensitive to incident angles [19]. In this paper, a new approach

is proposed to implement FSS structures with miniaturized elements and high selectivity.

The proposed FSS element is realized by using a resonant surface (the top side) and an inductive surface (the bottom side), as shown in Fig. 2. They are separated by a dielectric substrate with a thickness of *d*. The equivalent circuit of the proposed element is shown in Fig. 1(b). As shown in Fig. 2(a), the top layer of the proposed FSS is a resonant surface consisting of an inductive mesh and four capacitive patches as introduced in [19, 20]. The main physical features of the resonant surface in Fig. 2(a) can be described by the circuit model of Fig. 1. The corresponding equivalent component values for the resonant surface can be approximated based on the circuit theory in [21]. In the equivalent circuit, C_2 represents the capacitance between adjacent patches in one element, L_1 is the inductance of the outer square ring and C_1 is the mutual capacitance between adjacent elements.

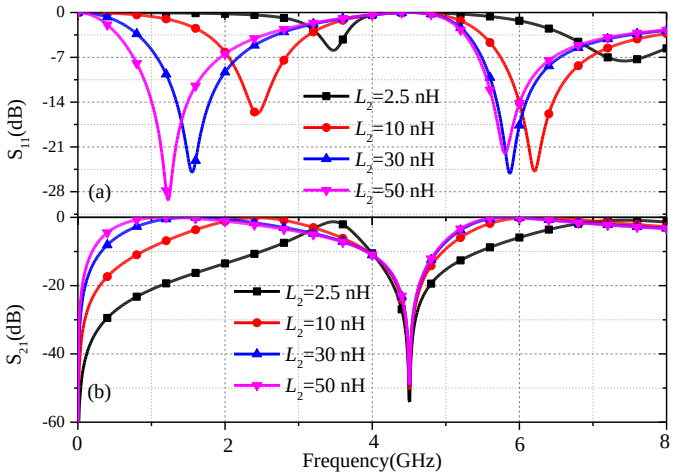

Fig. 4. The calculated (a) S_{11} and (b) S_{21} of the proposed FSS with the inductive layer of different inductances L_2.

The values of lumped-element components in Fig. 1 are approximately C_1=0.25, C_2=0.27 pF, L_1= 2.4 nH and L_2 = 2.5 nH. The calculated reflection and transmission coefficients of the equivalent circuit are shown in Fig. 3. It can be observed that the resonant surface has a passband at 5.7 GHz and stopband at 4.5 GHz. By adding the inductive layer, the inductance L_2 is introduced into the equivalent circuit as shown in Fig. 1(b). The passband frequency is shifted to 3.46 GHz and the resonant frequency of the stopband remains unchanged as shown in Fig. 3. The corresponding relative bandwidth of the 10-dB stopband at 4.5 GHz is widened from 18.5% to 31.2% while the passband bandwidth is significantly narrowed with the effect the inductance L_2.

In order to observe the influence of the inductance L_2 on S-parameters more clearly, the S-parameters for the equivalent circuit of the proposed FSS is calculated and illustrated as in Fig. 4 with different values of L_2. When the inductance L_2 is increased from 2.5 nH to 50 nH, the resonant frequency is shifted form 3.46 GHz to 1.2 GHz. The relative bandwidth is widened from 0 to 60.4%. When the passband and the stopband frequencies are close to each other, the FSS will achieve good selectivity.

The resonant surface, with the equivalent circuit shown in Fig. 1(a), has a bandpass response. This is determined by the equivalent circuit of L_1 in parallel with C_2. The impedance of the parallel circuit at frequency ω can be calculated by:

$$Z_p = j\omega L_1/(1-\left(\frac{\omega}{\omega_{0P}}\right)^2) \quad (3)$$

where

$$\omega_{0p} = 1/\sqrt{L_1 C_2} \quad (4)$$

is the resonant angular frequency of the parallel resonator. By connecting this *LC* parallel circuit with C_1 in series, it can easily calculate that the circuit will have both a stopband and a passband. It has a passband because at around the resonant frequency ω_{0p}, the parallel *LC* circuit has an impedance of infinity. The total impedance of C_1 in series with the *LC* circuit (L_1//C_2) is still close to infinity. Therefore the passband is maintained. At frequencies lower than the passband, the impedance of the parallel *LC* circuit, as can be calculated from (3), is inductive. This effective inductance in series with C_1 will form a series resonator, which will realize a stopband.

The proposed FSS can potentially be used as an AMC to improve the performance of antennas. This will be exploited in the future work. For such applications, the FSS will usually be attached to other material. For example, it can be used as RFID tags for IoT applications. If the FSS is attached to a dielectric material with a thickness of h_2, represented by Z_{ex} as shown in Fig. 1(b), the response of the FSS will be affected. This extra layer can be considered as a transmission line in a similar way to Z_d. The equivalent circuit model of the extra layer is composed of a series inductor (L_t) and a shunt capacitor (C_t), which can be obtained using the Telegrapher's model for TEM transmission lines [22].

In the proposed design, an inductive mesh layer, as shown in Fig. 2(b), is added on the other side of the substrate of Z_d. Since the stopband of the resonant FSS is mainly determined by L_1, C_1 and C_2 as shown in Fig. 1(a), the extra dielectric layer Z_{ex} and the inductive layer L_2 have little effect on the stopband frequency. It is because the effective impedance of the three components L_1, C_1 and C_2 is still close to zero at the stopband frequency, with or without L_2 and Z_{ex}.

This added inductive layer can improve the performance of the FSS on three aspects. Firstly, the added parallel inductance will significantly reduce the passband frequency of the FSS. This will effectively reduce the element size of the FSS element, making it insensitive to incident angles. In the original circuit as shown in Fig. 1(a), there is a passband because the circuit of L_1, C_1 and C_2 has a high input impedance of infinity at the resonant frequency ω_{0p} as defined in (4). By adding the inductive layer, with the influence of L_2, the input impedance is no longer high. As indicated in (3), the parallel circuit of L_1//C_2 is inductive at frequencies lower than frequency ω_{0p}. This effective impedance combined with L_2 and C_1 will resonate at a lower frequency, which will produce a passband. The passband frequency is much lower than that of the original FSS. Effectively, the element size is reduced very significantly.

Secondly, from the analysis above, it is obvious the stopband and the passband of the proposed FSS can be independently synthesized. The stopband is mainly determined of L_1, C_1 and C_2. The passband can be tuned by changing the value of L_2. The corresponding bandwidths can also be independently designed

by choosing the values of the four components properly. If the passband and the stopband are close to each other, the selectivity of the passband (or the stopband) can be significantly improved. Since both the transmitted wave and the reflected wave can be fed to the next stage, the FSS can potentially be used as a diplexer.

Thirdly, the inductance of the inductive layer will have a much stronger effect on the input impedance of the FSS than the extra layer of Z_{ex} as shown in Fig. 1(b). Thus, the extra transmission line has very little effect on the passband frequency. Furthermore, the response of mesh layer itself, being inductive surface, is not significantly influenced by surrounding dielectric materials. As a result, the overall performance of the FSS will be very insensitive to nearby dielectric materials. This feature is very useful for antenna applications when the FSS is attached to other materials.

To demonstrate the proposed design method, a prototype FSS was designed on a 1.6 mm thick FR4 substrate with a dielectric constant of 4.3. The geometry parameters after optimization are shown in Table I.

TABLE I

GEOMETRY PARAMETERS OF THE PROPOSED RESONANT SURFACE (unit:mm)

Parameter	D_x	D_y	h	W_l	W_s
Value	6	6	1.6	0.2	0.2
Parameter	W_i	W_p	ε_r	s	b
Value	0.2	2.3	4.3	0.1	0.2

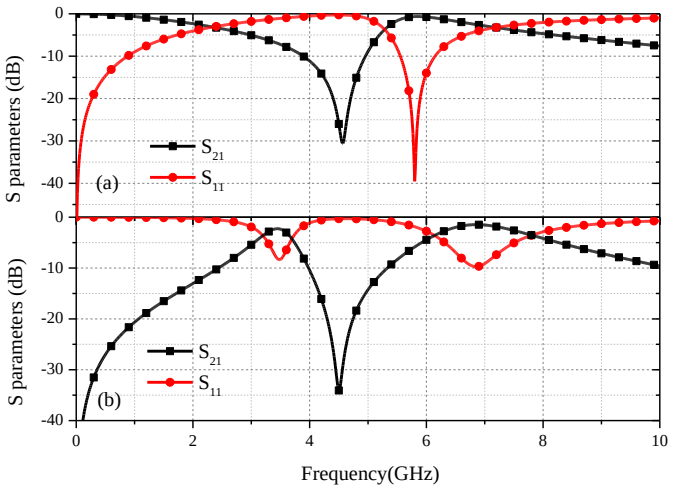

Fig. 5. The simulated S-parameters of (a) the original FSS without the inductive layer and (b) the proposed FSS with the inductive layer.

The S-parameters for the structure in the absence and presence of the inductive surface are simulated by CST. The results are illustrated in Fig. 5 (a) and (b), respectively. The passband frequency at 5.8 GHz of the original resonant surface is shifted own to 3.5 GHz when the inductive layer is added on the other side of the resonant surface. The corresponding bandwidth of the passband is changed as well, from 23.5% to 29.4%.

The proposed FSS with 3×3 array elements is shown in Fig. 6. To demonstrate the insensitivity of the proposed FSS to surrounding materials, the structure is simulated in four cases: the inductive layer is not attached to any dielectric material, attached to a 0.25 mm thick slab of Roger 3035 (RO3035) with ε_r = 3.5, Roger 3006 (RO3006) with ε_r = 6.15 and Roger 3210 (RO3210) slab with ε_r = 10.2. The simulated transmission coefficients over the frequency range from 0 to 10 GHz for the proposed FSS in the four cases mentioned above are shown in Fig. 7. When the dielectric constant of the additional dielectric materials is increased from 1.0 (no extra dielectric material) to 10.2 (RO3210), the four curves as illustrated in Fig. 7 are almost completely overlapping. This is because the change of the dielectric constant has little effect on the response of the proposed FSS. In order to observe the response more clearly, the transmission coefficient at the passband and the stopband are enlarged and embedded into Fig. 7. The stopband frequency is shifted from 4.5 GHz to 4.47 GHz when the dielectric constant of the attached material is increased from 1 to 10.2. The resonant frequency shift is less than 0.7%. The passband frequency changes no more than this.

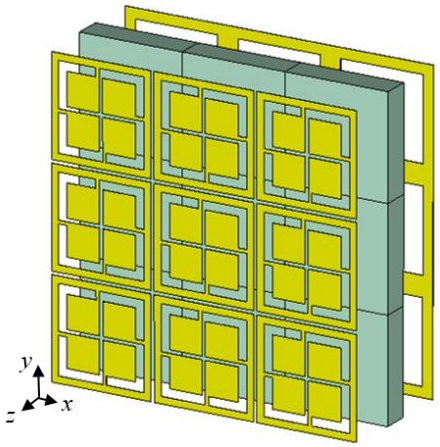

Fig. 6. Proposed FSS with 3×3 array elements.

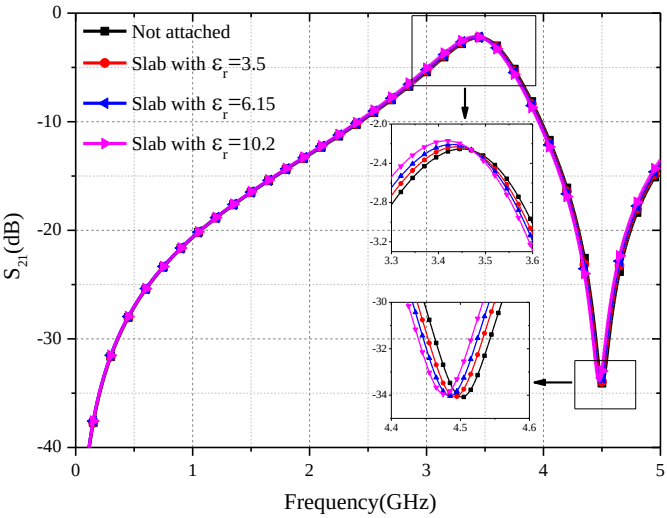

Fig. 7. Simulated transmission coefficients of the proposed structure when placed on 0.25 mm thick Roger slabs with dielectric constants ε_r = 3.5, 6.15 and 10.2, respectively. The stopband and passband details are enlarged and embedded in the figure.

To further observe the effect of the inductive layer on the response of the FSS, the S-parameters with inductive strip widths of W_i = 0.03, 0.1, 0.2 and 1.0 mm are simulated and shown in Fig. 8. As the strip width increases, the relative bandwidth of the passband decreases significantly and the passband edges become steeper. This indicates that the selectivity of the FSS can be enhanced by choosing the value of L_2. If any higher inductance value is desired, a thinner strip width or a meander line structure can be used.

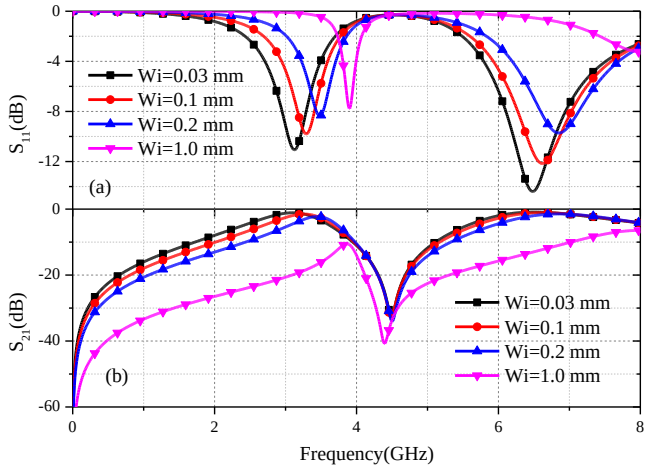

Fig. 8. Simulated transmission coefficients of the proposed FSS with different inductive strip widths of W_i=0.03 mm, 0.1 mm, 0.2 mm and 1.0 mm.

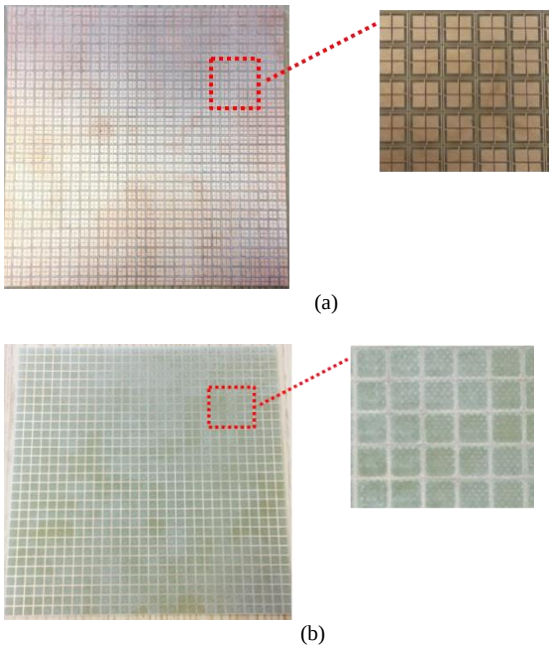

Fig. 9. A photograph of the fabricated prototype of the proposed FSS (a) the resonant surface and (b) the inductive surface.

IV. Experimental Results

An FSS consisting of 30 × 30 elements is fabricated on a 180 mm × 180 mm FR-4 substrate as shown in Fig. 9. Dimensions of the structure are summarized in Table I. The resonant surface (top side) is shown in Fig. 9(a), while the inductive surface (bottom side) is illustrated in Fig. 9(b). A vector network analyzer and two horn antennas are used for the measurement. The transmission coefficient between the two horn antennas was measured without the FSS, and then measured with the FSS between the antennas. Then, the measured transmission with the FSS is normalized with respect to the measured data without the FSS.

The prototype FSS is tested when it is attached to a 0.25 mm thick slab of Roger 3035 substrate (ε_r = 3.5), Roger 3006 (ε_r = 6.15) and Roger 3210 substrate (ε_r = 10.2). The experimental setup in an anechoic chamber is shown in Fig. 10. To compare the measured and simulated S_{21} more clearly, the curves of the measured S_{11} is shifted down by 0.279 GHz and shown in Fig. 11. It can be seen that the resonant frequency of the proposed FSS is very stable when the FSS is placed on different dielectric materials. The structure exhibits a passband at 3.5 GHz and a stopband at 4.5 GHz as designed.

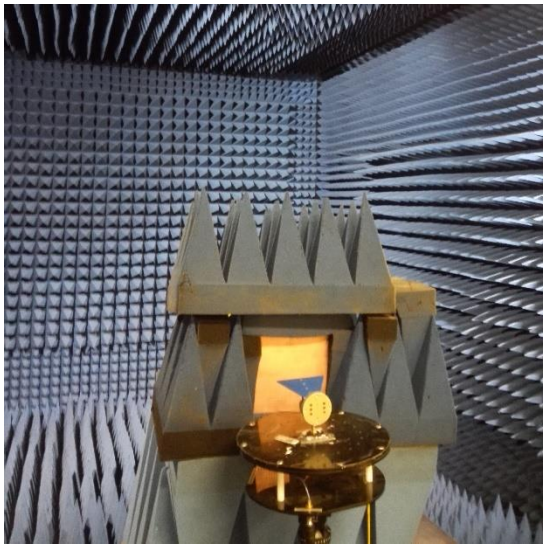

Fig. 10. Experimental setup in an anechoic chamber.

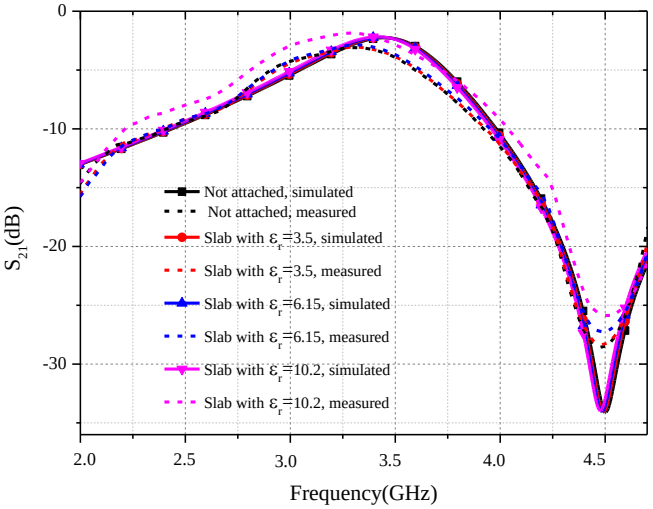

Fig. 11. Simulated and measured transmission coefficients of the proposed FSS when placed on a 0.25 mm thick dielectric slab with various dielectric constants (ε_r=3.5, 6.15, 10.2).

The FSS was also tested under various polarization angles, and the performance was also very stable (not shown here). The response of the FSS is the same for vertical and horizontal polarizations due to the symmetrical nature of the proposed element.

V. Conclusion and Future Work

In this paper, a study on the effect of an additional inductive surface on selectivity of frequency selective surfaces has been carried out. It has been demonstrated that, by combining a resonant surface and an inductive surface, the FSS can generate a passband and a stopband. The stopband performance is mainly determined by the resonant surface. The inductive layer can significantly lower the passband frequency, which effectively reduces the size of the FSS element. The passband response can be tuned by changing parameters of the inductive layer only. Thus the passband and the stopband can be independently synthesized.

The selectivity of the FSS can be improved by controlling the passband and stopband frequency and bandwidth. Theoretical and experimental results show that the performance of the FSS has been significantly improved by adding the inductive layer. The proposed FSS can be useful for many potential applications, which will be exploited in future work. For example, the proposed FSS can be used as a diplexer to separate signals at different frequency bands, or as a artificial magnetic conductor for antenna applications, to enable them achieving consistent performance when attached to various materials with arbitrary thicknesses.

References

[1] R. Ott, R. Kouyoumjian, and L. Peters, "Scattering by a Two-Dimensional Periodic Array of Narrow Plate," *Radio Science*, vol. 2, no. 11, pp. 1347-1359, Nov. 1967.

[2] B. Munk, and R. Luebbers, "Reflection properties of two-layer dipole arrays," *IEEE Transactions on Antennas and Propagation*, vol. 22, no. 6, pp. 766-773, Nov. 1974.

[3] R. Ulrich, "Far-Infrared Properties of Metallic Mesh and Its Complementary Structure," *Infrared Physics*, vol. 7, no. 1, pp. 37-&, 1967.

[4] C. Winnewisser, F. Lewen, and H. Helm, "Transmission characteristics of dichroic filters measured by THz time-domain spectroscopy," *Applied Physics a-Materials Science & Processing*, vol. 66, no. 6, pp. 593-598, Jun. 1998.

[5] S. Govindaswamy, J. East, F. Terry, E. Topsakal, J. L. Volakis, and G. I. Haddad, "Frequency-selective surface based bandpass filters in the near-infrared region," *Microwave and Optical Technology Letters*, vol. 41, no. 4, pp. 266-269, May 20, 2004.

[6] F. Bayatpur, and K. Sarabandi, "Single-layer high-order miniaturized-element frequency-selective surfaces," *IEEE Transactions on Microwave Theory and Techniques*, vol. 56, no. 4, pp. 774-781, Apr. 2008.

[7] B. Schoenlinner, A. Abbaspour-Tamijani, L. C. Kempel, and G. M. Rebeiz, "Switchable low-loss RF MEMS Ka-band frequency-selective surface," *IEEE Transactions on Microwave Theory and Techniques*, vol. 52, no. 11, pp. 2474-2481, Nov. 2004.

[8] D. Sievenpiper, L. J. Zhang, R. F. J. Broas, N. G. Alexopolous, and E. Yablonovitch, "High-impedance electromagnetic surfaces with a forbidden frequency band," *IEEE Transactions on Microwave Theory and Techniques*, vol. 47, no. 11, pp. 2059-2074, Nov. 1999.

[9] D. J. Kern, D. H. Werner, A. Monorchio, L. Lanuzza, and M. J. Wilhelm, "The design synthesis of multiband artificial magnetic conductors using high impedance frequency selective surfaces," *IEEE Transactions on Antennas and Propagation*, vol. 53, no. 1, pp. 8-17, Jan. 2005.

[10] H.-Y. Chen, and Y. Tao, "Performance improvement of a U-slot patch antenna using a dual-band frequency selective surface with modified Jerusalem cross elements," *IEEE Transactions on antennas and Propagation*, vol. 59, no. 9, pp. 3482-3486, 2011.

[11] B. Mandal, A. Chatterjee, and S. K. Parui, "A wearable button antenna with FSS superstrate for WLAN health care applications." *RF and Wireless Technologies for Biomedical and Healthcare Applications (IMWS-Bio), IEEE MTT-S International Microwave Workshop Series on* pp. 1-3. 2014.

[12] G.-Q. Luo, W. Hong, H.- J. Tang, and K. Wu, "High Performance Frequency Selective Surface Using Cascading Substrate Integrated Waveguide Cavities, " *IEEE Microwave and Wireless Components Letters*, vol. 16, no 12, Dec. 2006.

[13] F. Deng, X.-Q. Yi, and W.-J. Wu, "Design and Performance of a Double-Layer Miniaturized-Element Frequency Selective Surface, " *IEEE Antennas and Wireless Propagation Letters*, vol. 12, 721. 2013.

[14] M.-b. Yan, J.-F. Wang, H. Ma, S.-B. Qu, J.-Q. Zhang, C.-L.Xu, L. Zheng, and A.-X Zhang, " A Quad-Band Frequency Selective Surface With Highly Selective Characteristics, " *IEEE Antennas and Wireless Propagation Letters*, vol. 26, no. 8, Aug. 2016.

[15] D.-S. Wang, B.-J. Chen, and C.-H Chan, "High-Selectivity Bandpass Frequency-Selective Surface in Terahertz Band," *IEEE Transactions on Terahertz Science and Technology*, vol. 6, no. 2, Mar. 2016.

[16] M. Kartal, J. J. Golezani, and B. Doken, "A Triple Band Frequency Selective Surface Design for GSM Systems by Utilizing a Novel Synthetic Resonator," *IEEE Transactions on Antennas and Propagation*, vol. 65. no.5, May 2017.

[17] Y.-Q. Pang , Y.-F. Li, J.-Q. Zhang, Z. Xu, and S.-B. Qu, "Design of Frequency Selective Surface Based on Spoof Surface Plasmon Polariton Modes," *IEEE Antennas and Wireless Propagation Letters*, vol. 17, no 6, June 2018.

[18] M. Al-Joumayly, and Nader Behdad, "A New Technique for Design of Low-Profile, Second-Order, Bandpass Frequency Selective Surfaces, " *IEEE Transactions on Antennas and Propagation*, vol. 57, no. 2, Feb. 2009.

[19] M. N. Hussein, J. Zhou, Y. Huang, M. Kod, and A. P. Sohrab, "A Miniaturized Low-Profile Multilayer Frequency-Selective Surface Insensitive to Surrounding Dielectric Materials," *IEEE Transactions on Microwave Theory and Techniques*, 2017.

[20] M. Hussein, J. Zhou, Y. Huang, A. Sohrab, and M. Kod, "Frequency selective surface with simple configuration stepped-impedance elements." *10th European Conference on Antennas and Propagation (EuCAP)* pp. 1-4, 2016.

[21] N. Marcuvitz, *Waveguide handbook*: IET, 1951.

[22] W. R. Eisenstadt, and Y. Eo, "S-Parameter-Based IC Interconnect Transmission Line Characterization," *IEEE Transactions on Components, Hybrids, and Manufacturing Technology*, vol. 15, no. 4, Aug. 1992.